
THEORY AND PROCESSES OF FORMING AND SINTERING OF POWDER MATERIALS

Investigation into the Kinetics of Isothermal Sintering of Milled and Mechanically Alloyed Iron Powders

S. A. Oglezneva* and M. N. Portalov*

Perm National Research Polytechnic University, ul. Professora Pozdeeva 6, Perm, 614013 Russia

*e-mail: osa@pm.pstu.ac.ru

Received March 20, 2013; in final form, July 17, 2013; accepted for publication July 19, 2013

Abstract—The sintering kinetics is investigated and the activation energy of sintering of milled powders of iron and mechanically alloyed mixture “iron–0.5% carbon–5.6% ferrophosphorus” is calculated. The dislocation density increasing to 10^{11} cm^{-2} is calculated by X-ray phase analysis and metallography, and ordering of dislocations in milled powders of iron and mechanically alloyed mixture upon increasing the milling time is found. Based on the values of porosity, which vary during isothermal sintering at 900–1100°C in powders milled in different times, coefficients of the Ivensen equation and activation energy of sintering and concentration of structural defects, which are present in the beginning of isothermal sintering, are calculated. The results of investigations showed that the formation upon milling the dislocation structure with a high density of thermally unstable dislocations slightly activates sintering, and structural defects formed during the formation of solid solutions during mechanical alloying and heterodiffusion affect the activation of sintering much more strongly.

Keywords: iron powder, milling, mechanical alloying, dislocation structure, shrinkage, sintering kinetics, activation energy of sintering, Ivensen equation

DOI: 10.3103/S1067821215030153

INTRODUCTION

It is known that dispersed powders possess high activity to sintering [1, 2]. When sintering dispersed particles, the process moving force is the gradient of the thermodynamic potential, which is caused by the gradient of the concentration of vacancies that appears at curved surfaces. We can substantially vary the defect density of the crystal structure and surface curvature of powders upon milling the powders and thereby activate sintering.

Structural defects affecting the increased activity should possess stability in the high-temperature region, where the activity manifests itself. Such defects are dislocations and macroscopic defects of the type of interfaces between structural elements, pore surface, etc. [2]. It is known that porous compacts made of ultradispersed powders cannot be sintered to the low-porosity level. One cause of this is the fact that certain stoppers are overcome at low temperatures, while the remaining ones are insurmountable [2].

The description of the sintering kinetics is very complex in view of multitude of variables. However, the phenomenological description proposed by Ivensen, which is based on the continuously observed regularity of independence of the relative reduction of the porosity from the initial density of the powder body, is recognized as the most realistic one until now [3]:

$$V = V_i(qm\tau + 1)^{-1/m}, \quad (1)$$

where V and V_i are the pore volumes in the initial instant of sintering and in the beginning of isothermal holding; q is the constant, the physical sense of which is the rate of the relative reduction of the pore volume in the instant of the beginning of isothermal sintering; m is the constant that characterizes the intensity of lowering the reduction rate of the pore volume with the sintering time; and τ is the time of isothermal holding during sintering.

Among all known empirical equations, only this equation is able to describe both the rapid compaction in the first minutes of isothermal sintering and strongly retarded compaction after hours-long sintering; it is verified for powders of various metals and compounds.

We can establish the processes occurring at various stages of sintering by the values of equation constants.

When fabricating the powders using various methods, crystalline particles of powders differ not only by the total level of general imperfection, but also by the number of defects as well, which determines the main features of reduction of the porosity volume. It is established in computational studies of foreign researchers that, when milling the powders, the ratio of the number of mobile and immobile dislocations is determined by the material nature—hardness, melting point, and binding energy [4, 5]. The dislocation structure formed during milling will obligatorily affect sintering. When heating the powders with a high dislocation density, the annihilation rate of dislocations

rapidly decreases due to the retarding action of fastened dislocations against the motion of active dislocations. It is known that the activation energy is independent of temperature if it is calculated for one material having a definite type of active structural imperfections.

In terms of reasons of the phenomenological theory, active imperfections can form due to the coagulation of vacancies [3].

This study is targeted at investigating the influence of the microstructure of milled and mechanically alloyed iron powders on the kinetics and properties of powder materials and revealing the relation between the main parameters of sintering.

EXPERIMENTAL

Mechanical milling of the carbonyl iron powder of the VMS-1 grade was performed using a Pulverizette 4 planetary mill with a weight ratio of balls and powder of 30 : 1 for 0–100 h in argon (the ball diameter is 8 mm, ball material is steel ShKh15, cuvette diameter is 14 cm, orbital motion velocity is 284 rpm, and drum rotating velocity is 1298 rpm). Milled powders were compacted under a pressure of 500 MPa and sintered in hydrogen at 900–1100°C for 5 min, 1 h, and 2 h.

Mechanical alloying (MA) of the mixture of powders of iron (PZhr 2.200.28), carbon (0.5%), and ferrophosphorus (5.6%) was performed in a Kh38NOOT water-cooled planetary mill (orbital motion velocity is 700 rpm and drum rotating velocity is 1570 rpm) with a weight ratio of balls and powder of 30 : 1. The MA time was varied from 1 to 25 min.

The MA powders were compacted under a pressure of 700 MPa and sintered in hydrogen at temperatures of 900–1050°C for 5 min, 0.5 h, and 2 h. The density and porosity of the samples was measured after sintering. “Etching holes” were revealed in metallographic cross sections etched by a 2% solution of picric acid in ethanol [6].

The size distribution of conglomerates of powder particles and their shape were determined using an Analyzette 22 laser diffractometer. The average size of particles entering the composition of conglomerates was calculated based on the measurements of nitrogen adsorption over the specific surface of the powder (a Sorbi 4.0 device). The type and formation kinetics of point defects during crushing was judged by the variation in the interatomic distance established using a Shimadzu XRD 600 diffractometer. The distribution character of dislocations was analyzed by the broadening ratio of X-ray lines $k = \beta_{110}/\beta_{220}$: if k is close to the ratio of tangents of line angles, then the dislocation distribution is chaotic, and if it is close to the ratio of secants, then the dislocations form low-angle walls. In the case of the cellular dislocation distribution, their density was calculated by formula $\rho = 3/D^2$, where D is

the size of coherent scattering regions (CSR) for the chaotic distribution: $\rho = A\beta^2$, $A = 2 \times 10^{16} \text{ cm}^{-2}$.

To find constant m , we determined the ratio of pore volumes before (V_p) and after (V_s) sintering with the isothermal holding for 0 h (or 5 min), τ_1 and τ_2 .

Denoting $V_s/V_p = V_i$ for sintering for 0 h, V_1 for τ_1 , and V_2 for τ_2 , we calculated m for various sintering temperatures according to the formula:

$$\frac{(V_i/V_2)^m - 1}{(V_i/V_1)^m - 1} = \tau_2/\tau_1. \quad (2)$$

Constant q was found according to the equation

$$q = \frac{(V_i/V_1)^m - 1}{0.5m}. \quad (3)$$

We calculated the annihilation energy of imperfections (E_a) (further, the activation energy of sintering) as $1.5\Delta E$ [3], where $\Delta E = E_s - E_a$ and E_s is the activation energy of flow processes of the crystalline substance.

We calculated ΔE as follows:

$$\Delta E = \frac{\log m_1 - \log m_2}{T_1^{-1} - T_2^{-1}}, \quad (4)$$

where m_1 is the coefficient at temperature T_1 and m_2 —at T_2 .

We calculated for various temperatures

$$\alpha N_i = qm \exp E_a/(RT), \quad (5)$$

where N_i is the imperfection concentration in the beginning of isothermal sintering.

EXPERIMENTAL INVESTIGATION INTO THE STRUCTURE OF MILLED IRON PARTICLES

The influence of milling time (from 0 to 100 h) of the carbonyl iron powder (particles 3–10 μm in size) on the particle-size distribution (Table 1) is investigated. The experimental data show that the average sizes of conglomerates of particles (d_{av}) decrease with an increase in the crushing time, most intensely after milling for 32 h; such a character of decreasing the sizes can be associated with the accumulation of defects of the crystal structure. A small increase in d_{av} to 4 μm with the milling duration of 100 h can be caused by the appearance of nanodimensional particles liable to agglomeration. The granulometric composition contained about 10% nanoparticles with sizes smaller than 100 nm after 100-h milling.






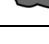
A continuous increase in the dislocation density in power to $\rho_1 = 21.79 \times 10^{10} \text{ cm}^{-2}$ after 100-h milling and an increase in the magnitude of microdistortions ($\Delta a/a$), most intense after 32 h, were observed during milling. The accumulation of defects of the crystal structure led to an increase in hardness and brittleness

Table 1. Microstructural characteristics of iron powders after milling

Milling duration, h	Average size of conglomerates of particles d_{av} , μm	CSR sizes D , nm	Microdistortions of crystal lattice $\Delta a/a$, %	Dislocation density ρ_1 , 10^{10} cm^{-2}	Dislocation distribution β_{110}/β_{220} *	Lattice parameter, \AA	
						a_{110}	a_{220}
5	6.3	100	—	1.0	0.35 (chaot.)	2.869	2.8670
32	5.8	95.28	0.043	3.3	0.30 (chaot.)	2.8728	2.8652
54	3.2	52.82	0.204	10.7	0.43 (bl.)	2.8626	2.8626
74	2.8	50.29	0.221	11.8	0.48 (bl.)	2.8515	2.8617
100	4.0	37.1	0.362	21.79	0.45 (bl.)	2.8748	2.8641

* The distribution is chaotic if β_{110}/β_{220} is closer to 0.251 and blocked if it is closer to 0.51.

Table 2. Shape of MA particles of iron-based mixtures

Milling duration, h	Apparent density, g/cm^3	Circle factor	Ellipsis factor	Roundness	Particle shape
0	1.8	1	1	1	
5	1.7	0.91	0.979	0.688	
32	1.5	0.78	0.941	0.69	
54	1.6	0.83	0.866	0.61	
74	1.4	0.974	0.992	0.77	
100	1.2	0.93	0.988	0.766	

of milled powder and promoted the destruction of particles and their conglomerates, as well as a decrease in d_{av} . The dislocation distribution ordered after 54-h milling. The failure mechanism of particles is preferentially friction, since the dislocation density considerably increased. The rain size in milled powders was 1 μm .

The shape of conglomerates of particles increasingly larger deviated from the ball with an increase in the milling time and was characterized by cut edges (Table 2). In addition, the intraparticle porosity formed when conglomerating the particles; this porosity and relief surface of conglomerates decreased the apparent density of the particles (the weight of freely poured powder in the volume unit responsible for the compaction of particles when pressing) (see Table 2).

The porosity of compacts under the more prolonged powder milling increased in connection with a decrease in the size of particles; rise of their microhardness; and, consequently, variation in the stressed state of powder particles [7].

The porosity of compacts made from milled powder particles reduced after sintering at 900 and 1100°C (Table 3).

EXPERIMENTAL INVESTIGATION INTO THE STRUCTURE OF MECHANICALLY ALLOYED MIXTURE OF POWDERS “IRON–CARBON–FERROPHOSPHORUS”

The spread iron powder has a spherical shape and sizes of 50–200 μm . Surface layers of iron particles are intensely bombarded by milling balls during the MA, which is accompanied by the incorporation of graphite and ferrophosphorus into the surface (Fig. 1a); microhardness of the surface light layer (ferrophosphorus) is 6150 MPa, and that of the internal part (alloyed ferrite) is 3600 MPa. It was revealed by optical microscopy that, by the end of the MA process, each particle of the composite under study represents a conglomerate, which includes multitude of finer (true) particles (Fig. 1b), the size of which, as was determined by the adsorption method, was 1–2 μm . The chemical composition of each particle leveled during the MA and the variation coefficient of the phosphorus concentration decreased following the exponential law from 0.16 to 0.02 with an increase in the alloying time. The CSR sizes of particles of iron–carbon–ferrophosphorus mixtures during milling were decreased to 20 nm, which is apparently the limiting value of D (Table 4). The CSR sizes also reduced to 16–25 nm under similar MA conditions of iron powder with chromium,

Table 3. Porosity before and after sintering the briquettes from milled iron powder

Milling duration, h	Compact porosity	Porosity after sintering under isothermal holding		
		5 min	1 h	2 h
Sintering temperature of 900°C				
5	0.425	0.375	0.31	0.284
32	0.43	0.364	0.31	0.281
54	0.43	0.35	0.30	0.277
100	0.448	0.38	0.317	0.287
Sintering temperature of 1100°C				
5	0.44	0.425	0.263	0.233
32	0.442	0.39	0.23	0.205
54	0.444	0.36	0.23	0.212
100	0.473	0.37	0.253	0.223

molybdenum, manganese, and carbon [8, 9]. It is known that the minimal grain (particle) size during milling or MA is determined by the material nature—hardness, melting point, binding energy, and ratio of the number of mobile and immobile dislocations [4]. For example, the minimal particle size after milling calculated for iron, which cannot be larger than the CSR size, is 8.1 nm according to the data [10].

The dislocation density increased during the MA from $\sim 1 \times 10^{10}$ to $\sim 2 \times 10^{11} \text{ cm}^{-2}$. Since the dislocation mobility decreases as the solid solution is formed and the dislocation density is increased [11], while the ordering of the mutual arrangement increases, the formation and growth of dislocation walls apparently occur due to blocking the dislocations at stoppers.

CALCULATION OF KINETIC PARAMETERS OF SINTERING OF MILLED AND MECHANICALLY ALLOWED POWDERS

The calculated coefficients of the Iverson equation for sintering the milled iron powder are presented in Table 5. Their analysis showed that a nonmonotonic (quasi-periodic) dependence of constant m on the sintering temperature is observed with an increase in the milling time. The activation energy of sintering is also nonmonotonic; in addition, it varies oppositely to m . The maximal values of constant q (the rate of relative reduction of the porosity volume to the initial instant of isothermal sintering) and αN_i (the imperfection concentration in the beginning of isothermal sintering) are attained for a milling time of 54 h, which can be associated with the formation of a sufficiently high density of mobile dislocations, which are still low-ordered. Coefficient m decreases with an increase in the sintering temperature of powders milled for 5 h, which is characteristic of metals. The value of m rises with an increase in temperature, which is caused by a complex shape of particles and gas pressure in intra-

particle pores. This fact should be taken into account when milling the powders with the addition of surfactants, which will be adsorbed during milling and isolate during sintering.

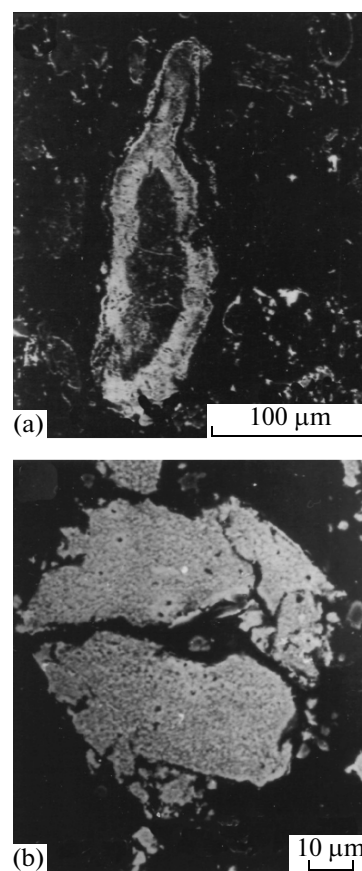

Fig. 1. Structure of particles of the iron–carbon–ferro-phosphorus MA mixture mechanically alloyed for (a) 1 min and (b) 25 min (etched).

Table 4. Microstructural characteristics of iron–carbon–ferrophosphorus powder mixture after milling

Milling duration, min	Average size of conglomerates of particles d_{av} , μm	CSR sizes D , nm	Dislocation density ρ_1 , cm^{-2}	Dislocation distribution β_{110}/β_{220}	Average particle size, μm	Particle number in conglomerate
0	35 ± 23	—	10^6	0.25 (chaot.)	1.4	20
1	13 ± 11	—	10^{10}	0.33 (chaot.)	1.0	13
5	12 ± 11	60	—	0.28 (chaot.)	0.6	20
10	11 ± 10	25	—	—	1.1	10
25	6 ± 4	20	2×10^{11}	0.44 (bl.)	0.4	15

Table 5. Coefficients of the Ivensen equation and activation energy of sintering for milled iron powder

Milling duration, min	q , h^{-1}	m	E_a , kJ/mol	αN_i , h^{-1}
Sintering temperature of 900°C				
5	0.33	5.0	27	1.65
32	0.34	2.0	69	0.68
54	0.60	4.1	42	2.50
100	0.38	2.0	51	0.76
Sintering temperature of 1000°C				
5	5.90	4.5	27	26.5
32	5.00	4.0	69	20.0
54	9.16	6.5	42	60.0
100	0.80	3.3	51	2.64

It was expected that the longer the milling time and the higher the density of dislocations and other defects are, the more active sintering will be; however, the powder milled for 54 h turned out to be most active. The shrinkage intensity in the case under consideration was caused by the maximal number of dislocations thermally stable to the beginning of sintering, which is confirmed by the highest value of αN_i .

The calculated activation energies of sintering of milled iron powders coincide in order of magnitude with the results of other authors and with our experimental data for other systems based on dispersed iron powders. For example, when sintering the iron powder

Table 6. Coefficients of the Ivensen equation and activation energy of sintering for milled iron powder

MA time, min	q , h^{-1}	m	E_a , kJ/mol	αN_i , h^{-1}
Sintering temperature of 1000°C				
25	1.9	1.2	240	3.08
1	0.84	9.0	257	7.56
Sintering temperature of 1050°C				
25	7.3	2.01	240	19.8
1	0.6	3.5	257	2.16

140 nm in size [12, 13], $E_a = 29\text{--}31$ kJ/mol; for the coarse-dispersed PZh3 powder, 51–58 kJ/mol, and for the carbonyl powder [3, 14], 196 kJ/mol. The activation energy of sintering the carbonyl iron powder with the addition of 14% of nickel nanopowder was 64 kJ/mol, while that of nanodimensional powders of the same composition was 34 kJ/mol [15, 16].

The observed variation in the magnitude of E_a during sintering depending on the milling time of iron powders is apparently mainly caused by the dislocation structure—the quality, number, and mobility of dislocations in powders milled for various times.

When calculating coefficients of the Ivensen equation for the MA system, it is established that, as the sintering temperature increases, the magnitude of m decreases for a mixture alloyed for 1 min and increases for a mixture alloyed for 25 min (Table 6). In the second case, this is associated with the presence of pores inside the conglomerates and an increase in the gas pressure in closed pores at the more uniform distribution of the liquid phase in a more dispersed system. The lack of mobile dislocations in the material under study was caused by the formation of the block dislocation structure after the MA.

The activation energy of sintering of powder steels mechanically alloyed with phosphorus and carbon was lower after the MA for 25 min and comparable in magnitude with the activation energy of sintering of carbonyl iron powders [12–16]. When comparing E_a of sintering of milled powders of iron and mechanically alloyed mixtures, it is seen that this quantity is independent of the time of milling or MA, but is determined by the type of the powder used: E_a for carbonyl powders is smaller by a factor of 3–8 compared with the mechanically allowed spread powder.

The value of αN_i after sintering in the solid phase at 1000°C was smaller in the system mechanically alloyed for 25 min; it is evident that even at a higher dislocation density and their high degree of ordering, the annihilation activity of defects is higher. Thus, heterodiffusion exerts no substantial effect on the activation of sintering for the sufficiently rapid heating to the temperature of solid-phase sintering.

Another situation is revealed at a sintering temperature of 1050°C: the value of αN_i is larger for the 25-min mixture than for the 1-min mixture (see Table 6).

In addition, the absolute concentration of imperfections in the 25-min mixture to the beginning of sintering at 1050°C is almost sevenfold higher than to the beginning of sintering at 1000°C. It is evident that the vacancy concentration abruptly increases to the beginning of liquid-phase sintering due to heterodiffusion. This concentration substantially exceeds the number of imperfections remaining to the beginning of sintering after the MA. Indeed, the calculated diffusivities in iron–ferrophosphorus diffusion pairs sintered at 900, 950, and 1000°C increase, while the width of the diffusion zone increases from 110 to 300 μm. Columnar grains elongated in the diffusion direction are formed in the structure of the diffusion zone at the side of iron during the liquid-phase sintering (Fig. 2). The dislocation zone revealed by the variation in microhardness turned out wider than the diffusion one, i.e., the diffusion was accompanied by the formation of dislocations [8]. The positive influence of the MA, which leads to an increase in dispersity and concentration of imperfections of powders, on the activation of sintering can be judged comparing not only the residual porosity (Table 7) but the magnitude of αN_i as well in the mixture alloyed for 1 min. The value of αN_i decreases as the sintering temperature increases (see Table 6), while the structural imperfections caused by heterodiffusion in the coarse-dispersed structure are still not formed to the beginning of sintering.

Thus, the defects formed when milling the powders turn out less stable to heating than the defects formed during the heterodiffusion. One more important conclusion follows from the comparison of the data of Tables 5 and 6: the activation of sintering is observed at the highest concentration of imperfections that are present in the beginning of sintering, and a certain degree of ordering of their distribution imparts stability to these imperfections.

INVESTIGATIONS INTO THE STRUCTURE AND PROPERTIES OF SINTERED MECHANICALLY ALLOYED PHOSPHOR STEELS

The strength for sintered steels increases with an increase in the ML duration from 1 to 25 min almost twice, while impact toughness and relative elongation increase by an order of magnitude (Fig. 3). The formation of the liquid phase additionally intensifies shrinkage and improves mechanical properties.

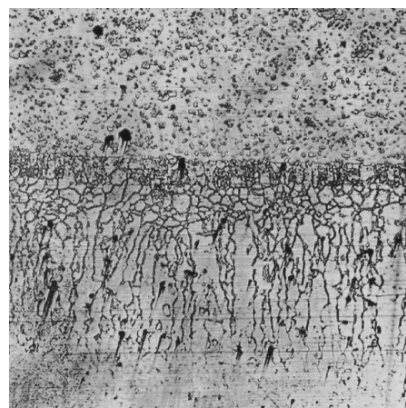


Fig. 2. Structure of the iron–ferrophosphorus diffusion zone sintered at 1000°C for 6 h, etched ($\times 400$).

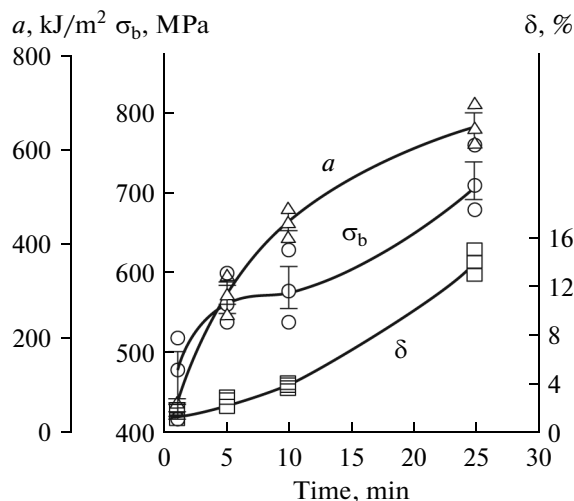


Fig. 3. Strength (σ_b), impact toughness (a), and relative elongation (δ) of sintered MA steel PK 50F depending on the MA duration.

MA-alloyed steels possess a porosity of 3–6%, grain size of 5–6 μm, ultimate strength up to 770 MPa, relative elongation up to 14%, impact toughness up to 700 kJ/m², and fracture toughness of 45–60 MN/m^{3/2}. The dislocation structure of the powder mixture prepared by the joint crushing of components promotes the activation of sintering and prevents the segregation of phosphorus at the boundaries during sintering; a microstructural analysis of sintered steels shows the formation of platelet steadite in steels without the MA (Fig. 4a) and

Table 7. Porosity before and after sintering of briquettes from the iron–carbon–ferrophosphorus powder mixture

Milling duration, min	Compact porosity	Sintering temperature, °C	Porosity after sintering under isothermal holding		
			5 min	0.5 h	2 h
1	0.25	1000	0.23	0.20	0.18
1	0.25	1050	0.21	0.18	0.10
25	0.40	1000	0.34	0.21	0.11
25	0.40	1050	0.25	0.11	0.60

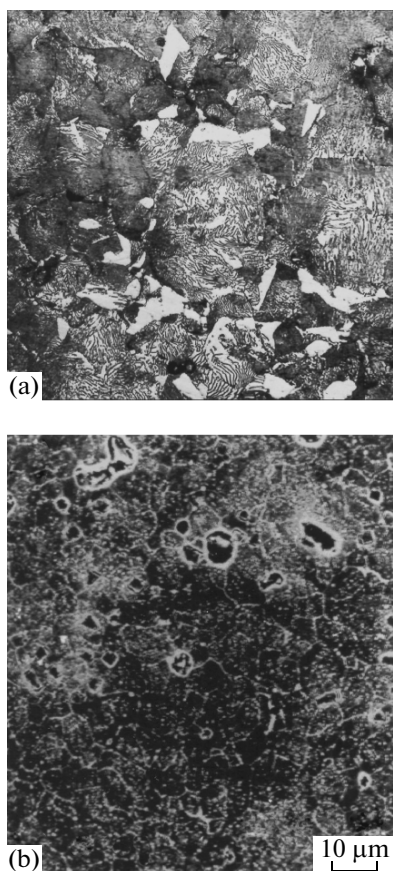


Fig. 4. Microstructure of sintered powder steels PK50F (etched). (a) MA time of 1 min and (b) 25 min. Magnification (a) $\times 200$ and (b) $\times 800$.

point distribution in MA steels (Fig. 4b). The dislocation density in the MA steel after sintering evaluated by the etching patterns on the metallographic cross section constitutes 10^9 cm^{-2} . In addition, certain ordering is retained in the dislocation distribution after sintering as well. Properties of MA phosphor steels, especially the relative elongation at a high strength, are better than those of analogs of powders PNC60 produced by Hoganas (Sweden) at a considerably lower temperature of activated sintering.

CONCLUSIONS

It is established based on the analysis of coefficients of the Ivensen equation, activation energy of sintering, and concentration of imperfections:

(i) The Ivensen equation describes well sintering in the iron–carbon–ferrophosphorus MA system.

(ii) Imperfections of the structure of the crystal lattice of iron formed during milling are thermally unstable and annihilate upon heating to the onset of isothermal holding; a high value of αN_i promotes the activation of sintering (both in the milled powder and in the mechanically activated system).

(iii) Structural imperfections formed during heterodiffusion rather than during milling promote the activation of sintering in the iron–carbon–ferrophosphorus system. It is established that mechanical alloying positively affects the activation of heterodiffusion and sintering.

(iv) The activation energy of sintering is not subjected to a substantial variation under the milling and MA of definite systems.

ACKNOWLEDGMENTS

This study was supported by the Russian Foundation for Basic Research, project nos. 10-08-00156_a and 12-08-31521_mol_a.

REFERENCES

1. Alymov, M.I., *Poroshkovaya metallurgiya nanokristallicheskikh materialov* (Powder Metallurgy of Nanocrystalline Materials), Moscow: Nauka, 2007.
2. Geguzin, Ya.E., *Fizika spevaniya* (Physics of Sintering), Moscow: Fizmatlit, 1984, 2nd ed.
3. Ivensen, V.A., *Fenomenologiya spevaniya i nekotorye voprosy teorii* (Phenomenology of Sintering and Certain Theoretical Questions), Moscow: Metallurgiya, 1985.
4. Mohamed, F.A., *Acta Mater.*, 2003, vol. 51, no. 14, p. 4107.
5. Mohamed, F.A. and Chauhan, M., *Metall. Mater. Trans. A*, 2006, vol. 37A, p. 3555.
6. Pshenichnov, Yu.P., *Vyavlenie tonkoi struktury kristallov: Spravochnik* (Revelation of a Fine Structure of Crystals: Handbook), Moscow: Metallurgiya, 1974.
7. Ignat'ev, I.E., Kontsevoi, Yu.V., Ignat'eva, E.V., and Pastukhov, E.A., *Izv. Vyssh. Uchebn. Zaved., Poroshk. Metall. Funkts. Pokryt.*, 2010, no. 3, p. 11.
8. Antsiferov, V.N., Bobrova, S.N., Oglezneva, S.A., et al., *Problemy poroshkovogo materialovedeniya* (Problems of Powder Materials Science), Yekaterinburg: Ural Branch, Russ. Acad. Sci., 2000, part 1.
9. Oglezneva, S.A., Mikhailov, A.O., and Zubko, I., *Izv. Vyssh. Uchebn. Zaved., Poroshk. Metall. Funkts. Pokryt.*, 2008, no. 2, p. 9.
10. Mohamed Farghalli, A. and Xun Yuwei, *Mater. Sci. Eng. A*, 2003, vol. 354, nos. 1–2, p. 133.
11. Grachev, S.V., Baraz, V.R., Bogatov, A.A., and Shveikin, V.P., *Fizicheskoe metallovedenie: Uchebnik dlya vuzov* (Physical Materials Science: Textbook for Higher School), Yekaterinburg: Ural State Tech. Univ.–Ural Polytech. Inst., 2001.
12. Matrenin, S.V., Il'in, A.P., Slosman, A.I., and Tolbanova, L.O., *Izv. Vyssh. Uchebn. Zaved., Poroshk. Metall. Funkts. Pokryt.*, 2009, no. 2, p. 11.
13. Matrenin, S.V., Il'in, A.P., Slosman, A.I., and Tolbanova, L.O., *Persp. Mater.*, 2008, no. 4, p. 81.
14. Skorokhod, V.V., *Reologicheskie osnovy teorii spevaniya* (Rheological Foundations of the Sintering Theory), Kiev: Naukova Dumka, 1972.
15. Oglezneva, S.A., *Russ. Metall. (Engl. Transl.)*, 2010, no. 1, p. 57.
16. Oglezneva, S.A., Bulanov, V.Ya., Kontsevoi, Yu.V., and Ignat'ev, I.E., *Metally*, 2012, no. 4, p. 115.

Translated by N. Korovin